A MATHEMATICAL MODEL FOR FRAZIL ICE EVOLUTION AND TRANSPORT IN CHANNELS

By Lars Hammar[1] and Hung Tao Shen[2]

ABSTRACT

A two-dimensional mathematical model for the formation and evolution of frazil ice in river channels is developed. The mean flow and transport in the channel is simulated by a $k - \varepsilon$ turbulence model.

In the simulation of the formation and evolution of frazil crystals, the primary nucleation is assumed to be due to the mass exchange of seeding crystals at the free surface. The size growth of frazil crystals is simulated based on the rate of heat transfer between each individual crystal and the ambient flow. The rate of heat transfer is a function of the particle size and the local turbulence intensity. A simplified secondary nucleation formulation is introduced to simulate the multiplication of frazil crystals in the flow.

The model is used to simulate the variation of water temperature during the frazil formation period and the evolution of size and concentration distributions of the frazil in the flow. Effects of the surface heat exchange rate and the rate of seeding in the channel are examined. The model will serve as the basis for the development of a model for the formation of anchor ice and the evolution of the surface ice runs.

[1]Research Engineer, Alvkarleby Laboratory, Vattenfall Engineering AB; and Doktorand, Lulea University of Technology, Lulea, Sweden

[2]Visiting Professor, Lulea University of Technology, Lulea, Sweden (on sabbatical leave from Clarkson University, Potsdam, NY, USA)

INTRODUCTION

The formation and evolution of frazil is one of the most important river ice phenomena during the freeze up period. The precise process of frazil evolution is not well understood. However, it is generally accepted that frazil forms in turbulent water when it is supercooled. The turbulence condition is necessary to effectively maintain the heat transfer from the river over its depth to the atmosphere. Turbulence is also required for the vertical entrainment of frazil crystals on the water surface to prevent the formation of static surface ice, which will inhibit the surface heat loss and the frazil production. In addition to turbulence and a small degree of supercooling, the presence of seed ice crystals is also required. These seed ice crystals or nuclei can come from a number of sources, including supercooled snow or ice particles and cold dust falling down to the water surface from the cold air, and ice particles from the border ice (Osterkemp 1978, Daly 1984). Once seeded, ice crystals will grow and multiply, in a dynamic balance between latent heat released by the growing ice crystals and heat exchanges with the atmosphere and the channel bed. The multiplication of frazil crystals is due to secondary nucleation. The secondary nucleation is caused by the shedding of small ice fragments from large frazil crystals when they collide with other particles or solid boundaries. The growth and multiplication processes generally cause the water temperature to rise to near 0° C to balance the latent heat released by frazil crystals.

Mathematical models have been used to simulate frazil and grease ice formation in surface waters (Omstedt 1985, Nyberg 1986). These studies show the potential use of numerical modeling technique to complement laboratory and field studies. In this paper, a two-dimensional model for the formation and evolution of frazil ice in river channels is developed. The model simulates the variation of water temperature and the evolution of size and concentration distributions of frazil in the flow. In the model the frazil ice formation is initiated by seeding small frazil nuclei on the water surface. The size distribution of the frazil is divided into ten groups. As the growth of the particles proceeds, concentrations in higher size groups increase. Secondary nucleation is simulated by converting the mass of growth in the highest size group into new frazil crystals of the size of the smallest size group. The mechanism of collisions between frazil particles is not considered. Sample simulations are presented. Effects of the surface heat exchange, the rate of seeding, and the flow condition are examined. The model will later serve as the basis for the development of a model for the formation of anchor ice and the evolution of surface ice runs.

MATHEMATICAL FORMULATION

The mathematical model is based on the PHOENICS code, which is a general purpose equation solver for heat and mass transfer problems (Spalding 1981). The PHOENICS code is applicable to general three dimensional unsteady flow simulations with irregular boundaries. The present study is, however, limited to two-dimensional steady state flows along a straight channel of infinite width. A standard $k - \varepsilon$ turbulence model is used in the flow simulation. The frazil crystals are assumed to be thin circular plates with a constant ratio of 1/10 between thickness and diameter. This thickness to diameter ratio is selected based on the measurements obtained from a laboratory flume by Daly and Colbeck (1986). The size distribution of the frazil crystals is described by ten size groups represented by their mean diameters. Seeded crystals as well as those produced by secondary nucleation are assumed to be in the lowest size group.

Mean Flow Equations

The mean flow and the transport in the channel are simulated by the following governing equations, along with a standard $k - \varepsilon$ turbulence model.

$$\frac{\partial U_i}{\partial t} + U_j \frac{\partial U_i}{\partial x_j} = -\frac{1}{\rho}\frac{\partial P}{\partial x_i} + \frac{\partial}{\partial x_j}(\nu_t \frac{\partial U_i}{\partial x_j}) + g_i \tag{1}$$

$$\frac{\partial T}{\partial t} + U_i \frac{\partial T}{\partial x_i} = \frac{\partial}{\partial x_i}(\frac{\nu_t}{\sigma_t}\frac{\partial T}{\partial x_i}) - S_b + S_f \tag{2}$$

$$\frac{\partial C_k}{\partial t} + U_i \frac{\partial C_k}{\partial x_i} = \frac{\partial}{\partial x_i}(\frac{\nu_t}{\sigma_c}\frac{\partial C_k}{\partial x_i}) - \omega_k \frac{\partial C_k}{d x_2} + S_{C_k} \tag{3}$$

in which ρ = density of the mixture, $\rho_w + (\rho_i - \rho_w)\sum_k C_k$; U_i = ith component of the mean velocity; P = pressure; ν_t = kinematic eddy viscosity; g_i = ith gravity component; σ_t and σ_C = Prandtl/Schmidt numbers; T = water temperature; C_k = volumetric concentration of frazil in the kth size fraction; ω_k = buoyant velocity of frazil, S_b and S_f = source terms due to the heat loss at the channel boundaries and the heat gain due to frazil growth, and S_c = a source term due to frazil production.

Frazil Evolution

The frazil ice size distribution is divided into 10 size groups represented by their respect mean diameters. The sizes of these groups range from 0 - 0.5 mm to 4.5 - 5.0 mm size intervals. Seed crystals and secondary nuclei are assumed to be in the 0 - 0.5 mm size group.

The rate of growth of an ice crystal depends on the rate of transfer of latent heat from the crystal to the ambient turbulent flow. The rate of heat transfer per unit ice area, q, can be expressed in terms of the heat transfer coefficient, h, as:

$$q = h(T_i - T_w) \tag{4}$$

where, T_i is ice surface temperature and T_w is the ambient water temperature. The heat transfer coefficient, h, can be expressed in its dimensionless form as a Nusselt number defined by:

$$N_u = \frac{h\ell}{k_w} \tag{5}$$

where, ℓ, is a characteristic length of the ice crystal, and k_w is the thermal conductivity of water. The characteristic length is chosen to be the thickness of the ice particle, since the main heat transfer takes place on the edge of the particle.

Combining Eqs. 4 and 5 gives the following equation for the rate of heat transfer:

$$q = \frac{N_u k_w}{d_e}(T_i - T_w) \tag{6}$$

where, d_e is the thickness of the ice particle.

The Nusselt number depends on the flow condition and the suspended particle size. In this study, the following formulation developed by Batchelor (1980) and Wadia (1974), as summarized by Daly (1984) is used:

For small particles:

$$N_u = (\frac{1}{m^*}) + 0.17P_r^{\frac{1}{2}} \quad ; \text{ if } m^* < \frac{1}{(P_r)^{\frac{1}{2}}} \tag{7a}$$

and,

$$N_u = [(\frac{1}{m^*}) + 0.55(\frac{P_r}{m^*})^{\frac{1}{3}}] \quad ; \text{ if } \frac{1}{(P_r)^{\frac{1}{2}}} < m^* < 10 \tag{7b}$$

in which, $m^* = r/\eta$, is the ratio between the radius of the ice crystal and the Kolmogorov length scale.

For large particles, i.e. $m^* > 1$,

$$N_u = 1.1 \;\; [(\frac{1}{m^*}) + 0.80\alpha_T^{0.035}(\frac{P_r}{m^*})^{\frac{1}{3}}] \quad ; \text{ if } \alpha_T m^{*\frac{4}{3}} < 1000 \tag{8a}$$

and,

$$N_u = 1.1 \;\; [(\frac{1}{m^*}) + 0.80\alpha_T^{0.24}P_r^{\frac{1}{3}}] \quad ; \text{ if } \alpha_T m^{*\frac{4}{3}} > 1000 \tag{8b}$$

in which, $\alpha_T = \sqrt{\overline{u^2}}/\bar{U}$, is the turbulence intensity. In the transition region, i.e. $1 < m^* < 10$, the variation of N_u is not well defined. In this study, Eq. 8 is used when $m^* > 1$.

Based on the above formulation, the source term, S_f, due to frazil growth, in Eq. 2, and the corresponding source term, S_{C_k}, in Eq. 3 can be determined. The term S_f can be written as:

$$S_f = \sum_k C_k q_k (d_{f_k}\rho_w C_p)^{-1} \tag{9}$$

where, d_{f_k} is the mean face diameter of particles in the kth size group. Correspondingly, the rate of thermal growth of ice mass in the kth size group is:

$$S_k = 4C_k q_k (d_{f_k}\rho_f L)^{-1} \tag{10}$$

where, L is the latent heat of fusion of ice. The net increase in ice concentration in the kth size group then becomes

$$S_{C_k} = (\frac{S_{k-1}}{\Delta\nu_{k-1}^p} - \frac{S_k}{\Delta\nu_k^p})\nu_k^p \tag{11}$$

in which, ν_k^p is the volume of a single ice particle in the kth size group, and $\Delta\nu_k^p = \nu_{k+1}^p - \nu_k^p$. The term on the right-hand side of Eq. 11 represents the increase in C_k, contributed to by the growth in the $(k-1)$th size group, and the decrease in C_k due to the growth in the kth size group. The growth in the largest particle size group is treated as a source for secondary nucleation, and is moved into the lowest size group accordingly. This means that

$$S_{C_1} = S_{10} - \frac{S_1}{\Delta \nu_1^p} \nu_1^p \tag{12}$$

and

$$S_{C_{10}} = \frac{S_9}{\Delta \nu_9^p} \nu_{10}^p \tag{13}$$

The buoyant velocity in the concentration equation is modelled by a simple Stokes' formula (Ashton 1983):

$$\omega_k = \frac{g d_{eq}^2}{18 K \nu} \left(\frac{\rho_w - \rho_i}{\rho_w} \right) \tag{14}$$

where, d_{eq} is the equivalent diameter defined as the diameter of a sphere having the same volume of the disc, and K is the resistance factor and is assumed to have a constant value of 2 for simplicity.

RESULTS

Four examples are presented to demonstrate effects of seeding and heat exchange rates on the evolution of frazil size, temperature and concentration distributions in a channel.

Case 1. In this example, the simulation is carried out for a 2 km long reach of an open channel. The reach is discretized into 200 x 10 cells. The seeding rate is 10^{-5} kg/(m^{2}s) on the surface of a 200 m long reach at the upstream end. Heat loss to the atmosphere is 500 W/m^2 along the entire reach. The flow in the channel is steady uniform, with a bed roughness height of 0.3 m. The mean flow velocity is 0.554 m/sec., and the flow depth is 5 m.

Figure 1 shows variations of the depth-average concentrations in each size group C_I and the normalized values C_I/C_{sum}, along the channel. The depth-averaged concentration C_I is defined as $\int u c_i dy / \int u dy$, and $C_{sum} = \sum_{I=1}^{10} C_I$. These figures shows that the relative concentration in the lowest size group reduces rapidly and the size distribution curves slowly shift toward larger sizes. A simple analysis of the heat transfer rate indicated that it will take from 10^4 to 10^6 seconds to grow a seed ice crystal to the largest crystal size. Figure 2 shows the vertical distribution of water temperature and concentration distributions of different size groups at 1000 m and 2000 m from the upstream boundary. The water temperature is normalized by the depth averaged water temperature $\bar{T}_w$. As expected, larger size particles tend to concentrate to the water surface. The variation of the depth-averaged water temperature is shown in Fig. 9. Distributions of turbulence quantities are shown in Fig. 10.

Case 2. This example simulates the same condition as in Case 1, except that the seeding rate is reduced to $10^{-7} kg/(m^2 s)$. The results of this simulation, are shown in figures 3 and 4. Figure 3 shows that the total concentration is smaller than that of Case 1, but the relative concentration of large ice crystals is higher. A larger supercooling is observed in Fig. 9. A comparison of relative size distribution curves in Fig. 3 and the water temperature curve in Fig. 9 shows that at a distance of about 1200 m from the upstream end the size distribution curve reaches a constant shape. At the same time the supercooled water temperature recovers from it's maximum value. This indicates that the surface heat loss is more effectively compensated by the ice growth when the number of large size particles increases. This is mainly due to the fact that large size particles tends to concentrate toward the water surface, where the heat loss takes place. The growth in largest size particles contributes to the formation of small crystals through secondary nucleation. These small particles are then mixed into the deeper part of the water to grow and balance the supercooling in the lower layer. The above discussion shows the complexity of the frazil evolution process and the importance of turbulence characteristics of the flow.

Case 3. This example is the same as Case 1, except that the heat loss rate is reduced to $250W/m^2$. Results presented in figures 5, 6 and 9 show that both the degree of supercooling and concentrations are reduced. The concentration in size groups 9 and 10 are very small.

Case 4. This example is the same as Case 1, except that an additional 2000 m long ice covered reach is added to the simulation at the downstream end. The result of this simulation is shown in Figs. 7 to 8. Figures 8 and 9 show that the water temperature begins to recover once it enters the ice covered reach. The rate of ice growth also diminishes, especially for large size particles. These are caused by the elimination of the surface heat loss by the ice cover and the higher concentration of large size particles in the upper layer of the flow.

In all cases the size distribution approaches the Gaussian distribution, but slightly skewed toward larger sizes. This skewness is due to the fact that seeding occurs only over a short reach at the upstream end. The Gaussian type size distribution has been observed in the laboratory by Daly and Colbeck (1986).

CONCLUSIONS

In this paper, the development of a two-dimensional mathematical model for frazil evolution in river channels is presented. A few simulation examples are given to illustrate variations of water temperature, concentration and particle size distributions. Several shortcomings of the model exist. These include: a) large scale secondary circulation, which almost always exists in real channels, is not taken into account; b) the interference of neighboring particles on heat transfer from frazil particles are not considered; c) flocculation and the mechanism of secondary nucleation due to particle collisions needs to be considered d) the model needs to be extended to include formations of static surface ice and surface ice runs; e) the effect of frazil particles on the flow, especially in high concentration regions, should be considered; f) the model needs to consider the size dependency on the Prandtl/Schmidt number for particles, i.e. larger particles tend to travel with the mean flow, instead of with the turbulent fluctuations, due to the inertia effect. Improvements are planned for some of the above. Yet some others still require further research, due to the lack of fundamental understandings in the state-of-the-art in these areas.

ACKNOWLEDGEMENTS

The second author would like to acknowledge the support provided by the Swedish Natural Science Research Council for his sabbatical leave at the Lulea University of Technology.

REFERENCES

Ashton, G.D. (1983) "Frazil Ice," in *Theory of Dispersed Multiphase Flow*, Academic Press, Inc., pp. 271-289.

Batchelor, G.K. (1980) "Mass Tranfer from Small Particles Suspended in Turbulent Fluid," *Journal of Fluid Mechanics*, 98[3], pp. 609-623.

Daly, S.F. (1984) Frazil Ice Dynamics, *CRREL Monograph 84-1*, USA Cold Regions Research and Engineering Laboratory, Hanover, NH.

Daly, S.F., and Colbeck, S. (1986) "Frazil Ice Measurements in CRREL's Flume Facility," *IAHR Symposium on Ice*, Iowa City, IA.

Nyberg, L. (1986) "Ice Formation in Rivers," *Numerical Simulation of Fluid Flow and heat/Mass Transfer Processes*, C.A. Barabbia and S.A. Orszag, ed., Springer-Verlag.

Omstedt, A. (1985) "Modelling Frazil Ice and Grease Ice in the Upper Layers of the Ocean," *Cold Regions Science and Technology*, 11, pp. 87-98.

Osterkemp, T. (1978) "Frazil Ice Formation: A Review," *Journal of Hydraulics Division*, ASCE, 104[HY9], pp. 1239-1255.

Spalding, D.B. (1981) "A General Purpose Compute Program for Multi-dimensional One- and Two-Phase Flow," *Mathematics and Computers in Simulation*, XXIII, North-Holland Publishing Co., pp. 267-276.

Wadia,P.H. (1974) Mass Transfer from Spheres and Discs in Turbulent Agitated Vessels, *Ph.D. Dissertation*, Department of Chemical Engineering, Massachusetts Institute of Technology, Cambridge, MA.

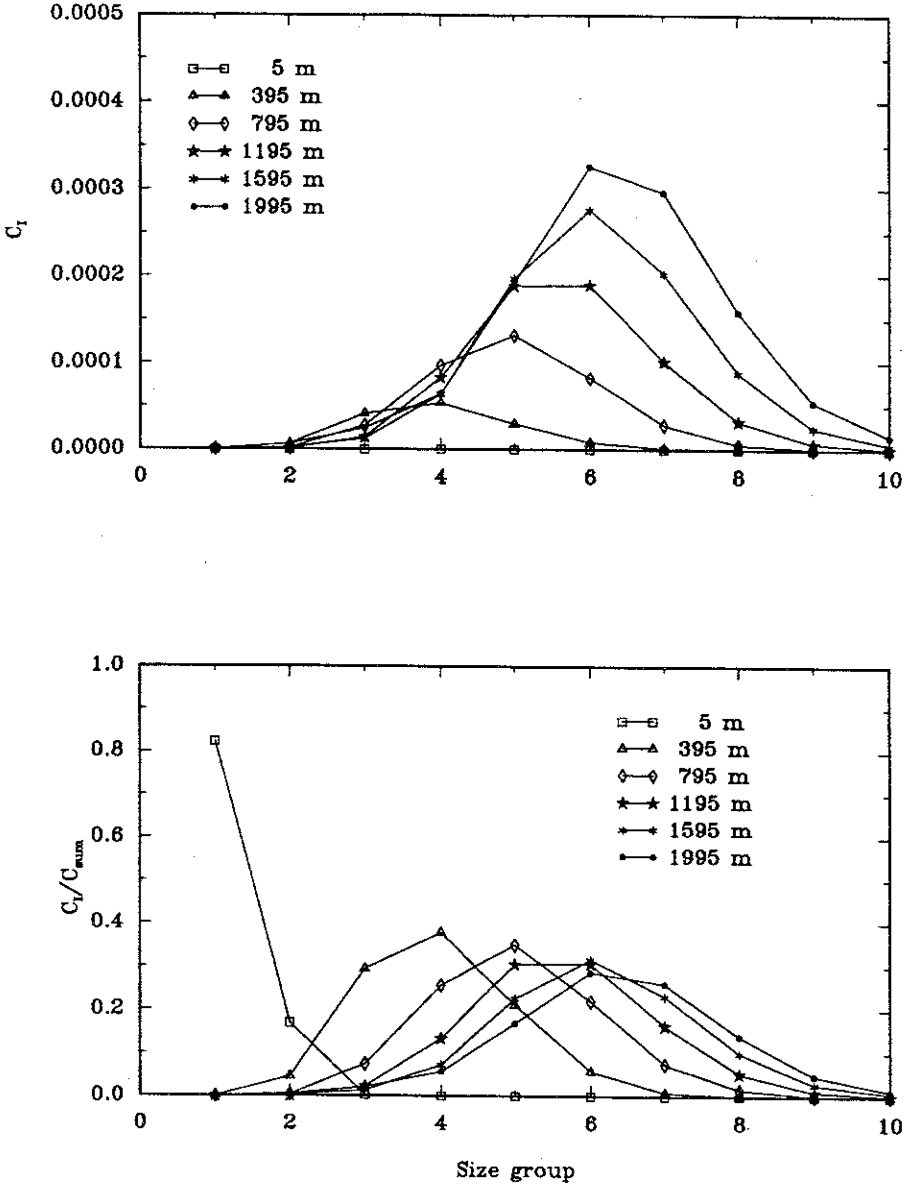

Figure 1: Evolution of ice crystal sizes along the channel, Case 1.

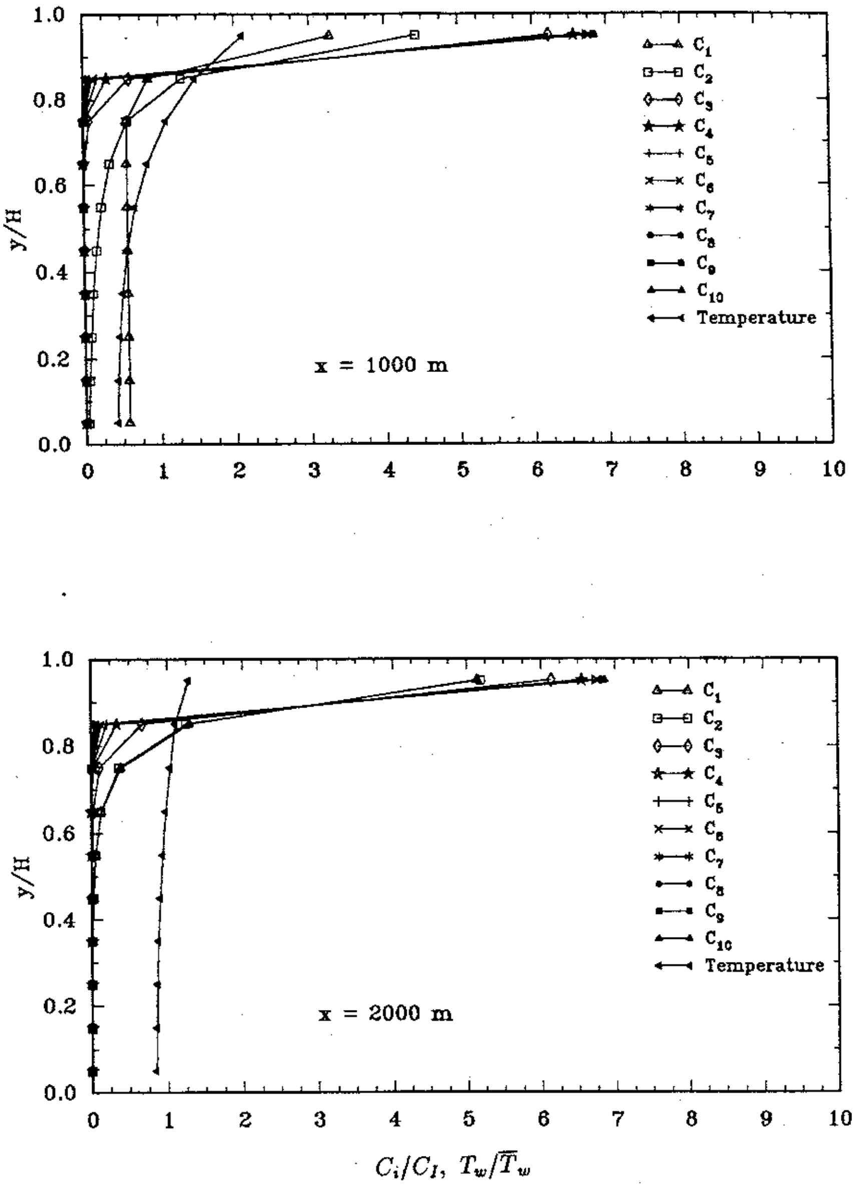

Figure 2: Normalized concentration and water temperature profiles, Case 1.

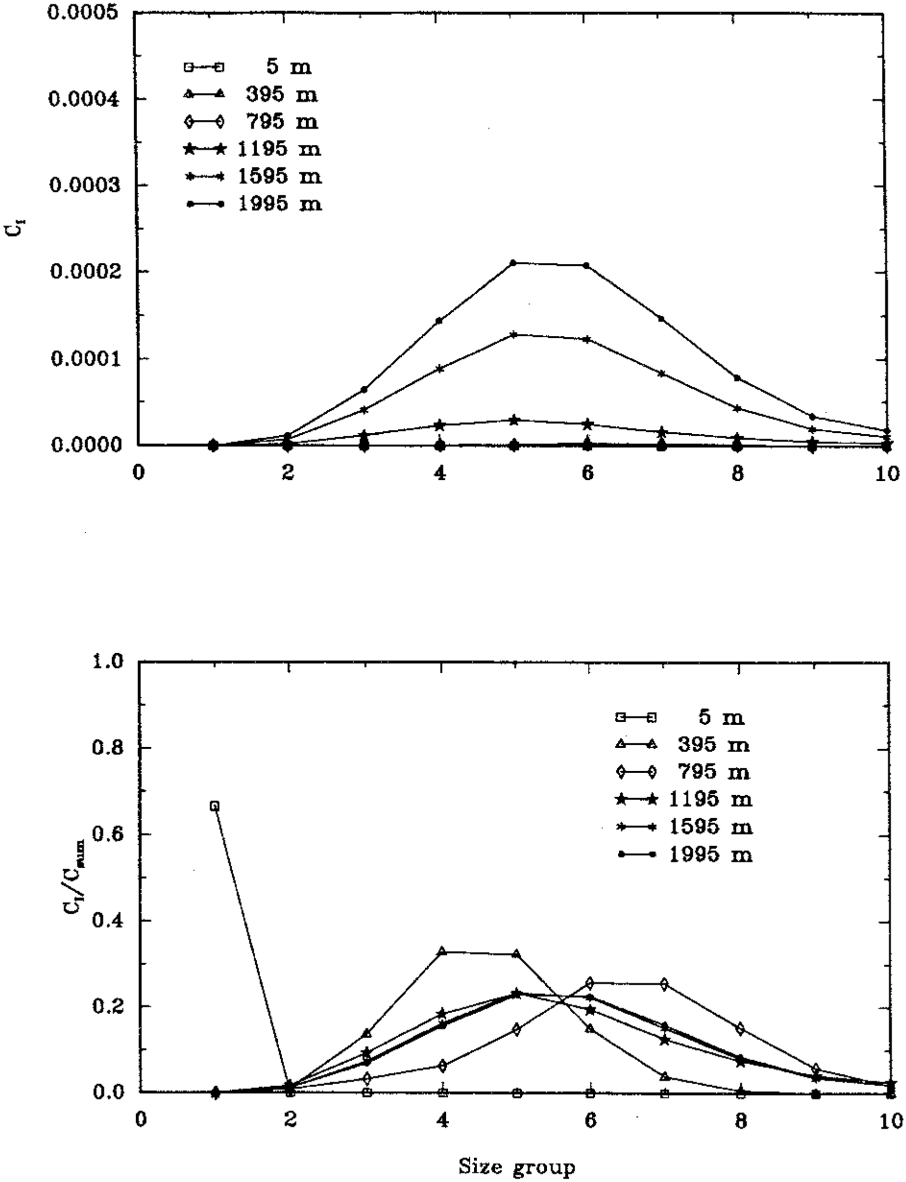

Figure 3: Evolution of ice crystal sizes along the channel, Case 2.

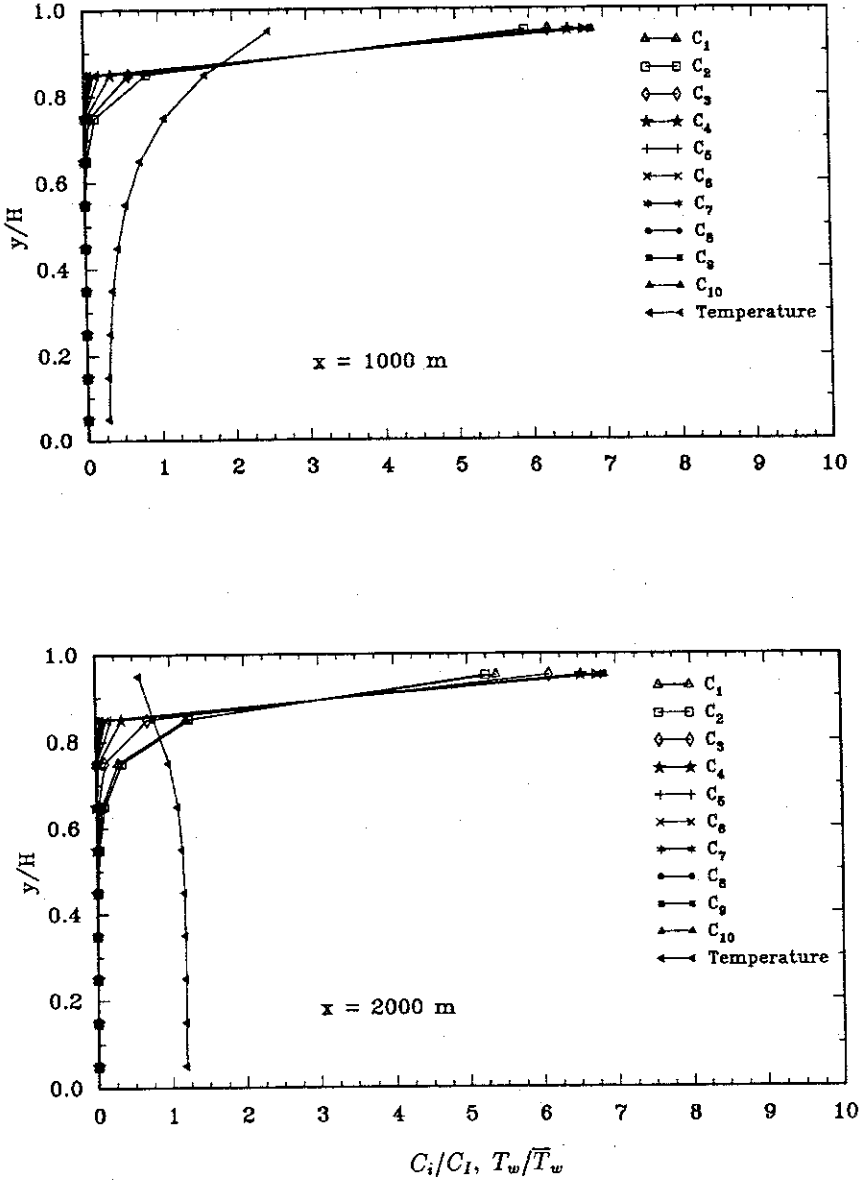

Figure 4: Normalized concentration and water temperature profiles, Case 2.

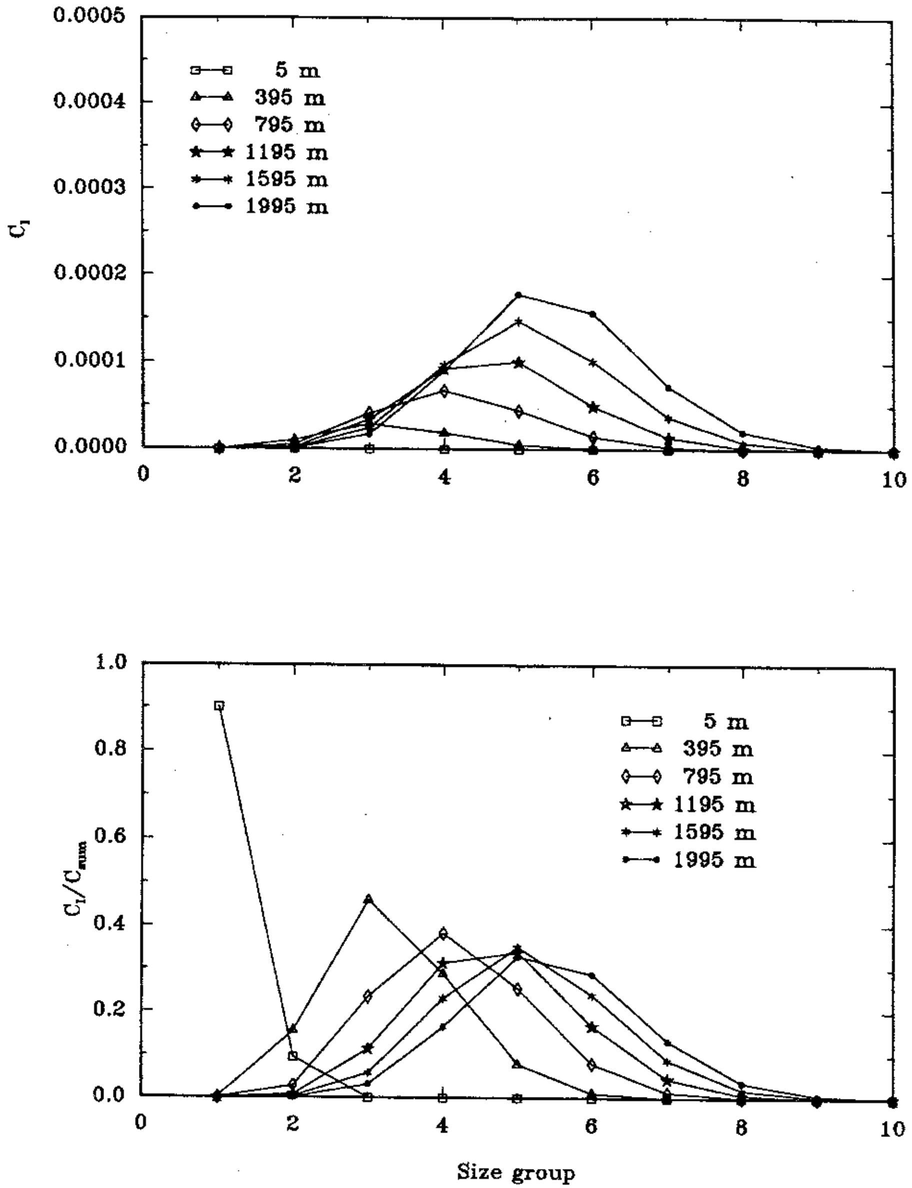

Figure 5: Evolution of ice crystal sizes along the channel, Case 3.

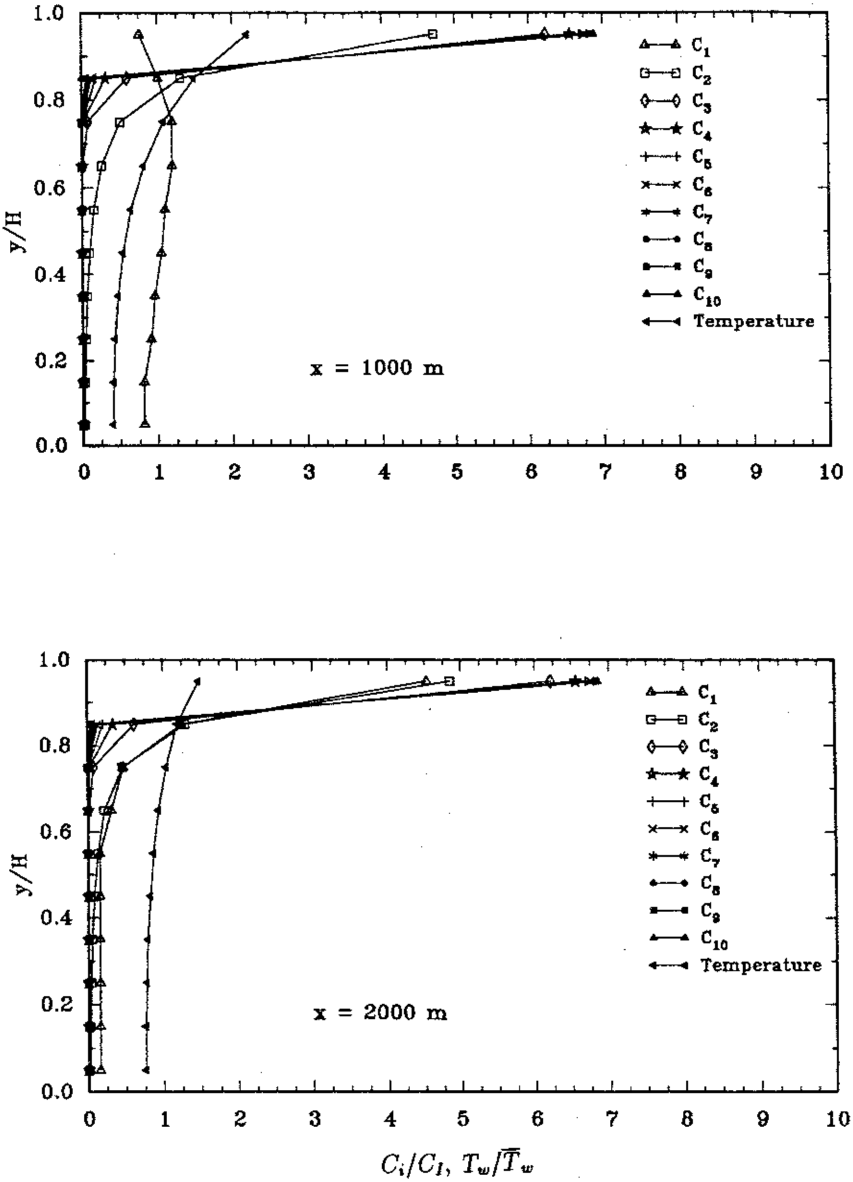

Figure 6: Normalized concentration and water temperature distributions, Case 3.

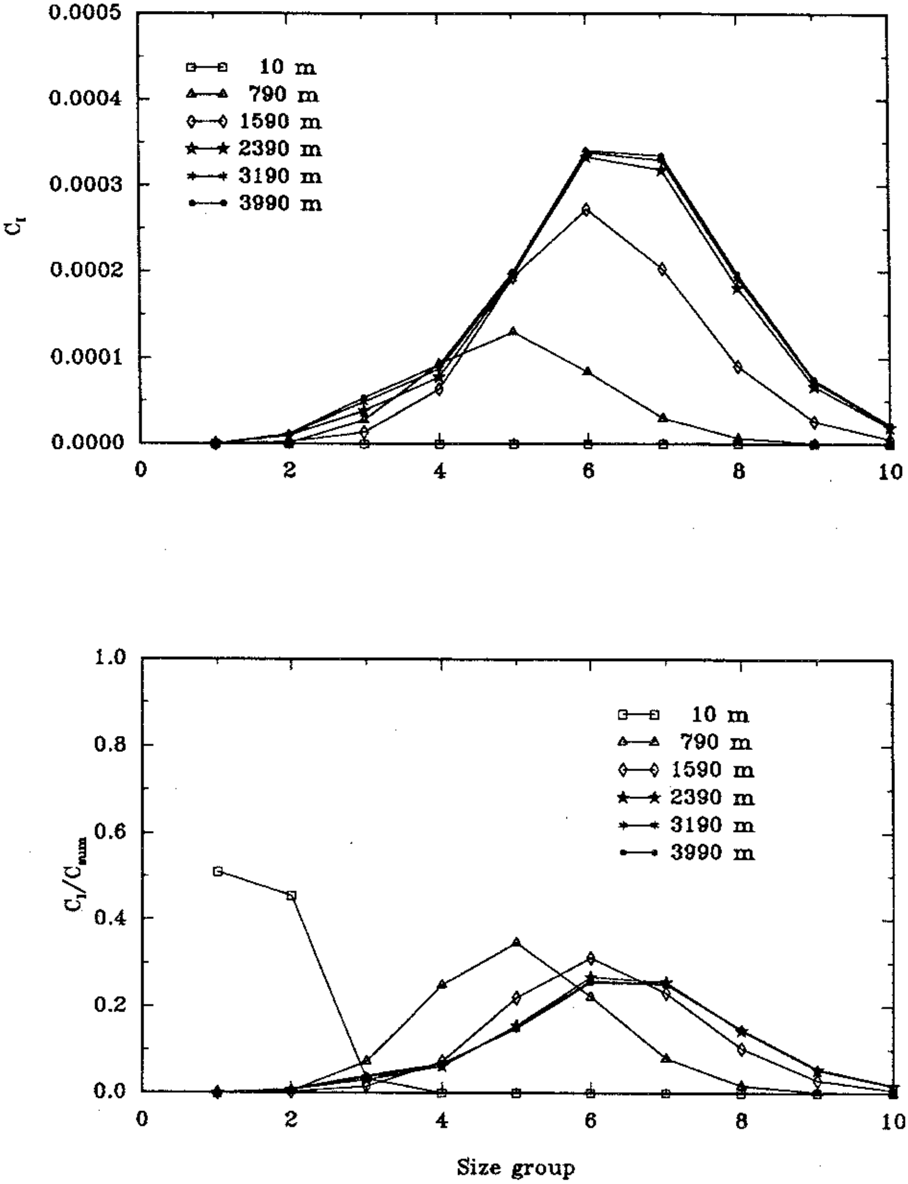

Figure 7: Evolution of ice crystal sizes along the channel, Case 4.

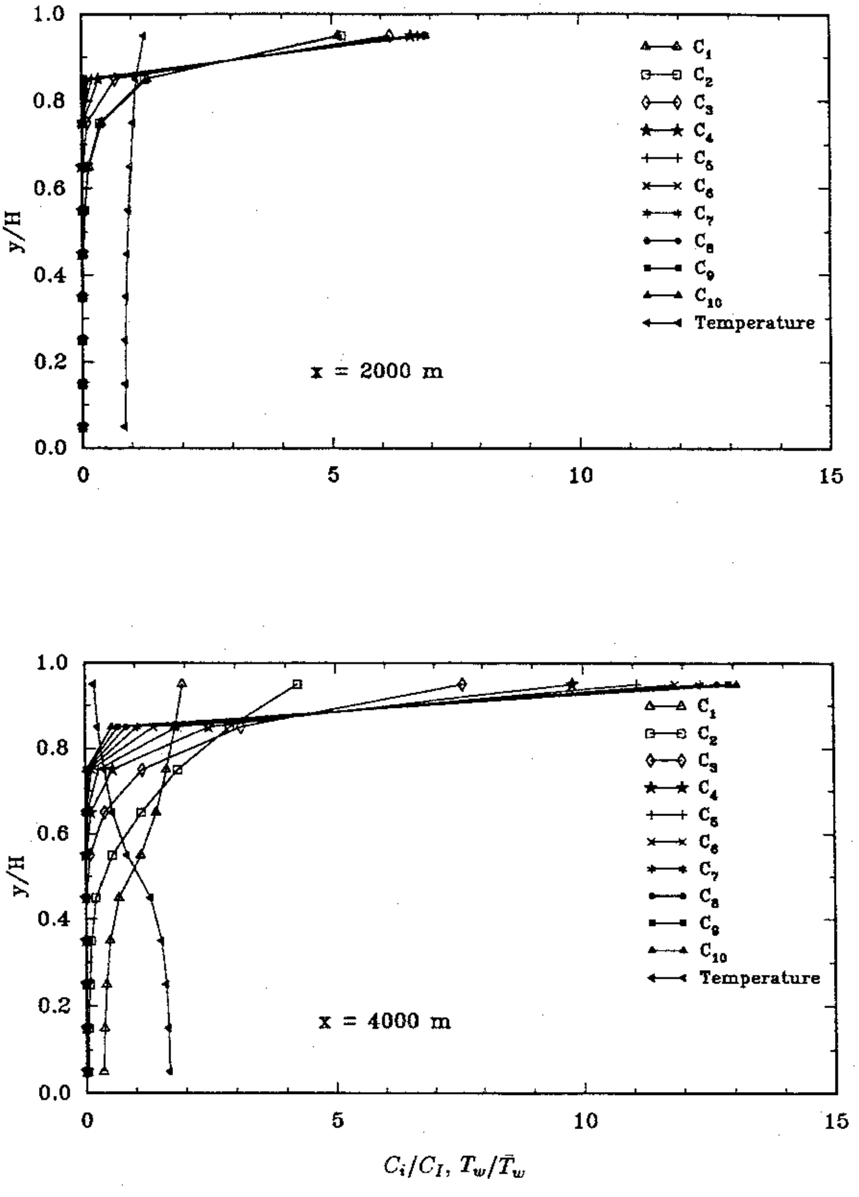

Figure 8: Normalized concentration and water temperature distributions, Case 4.

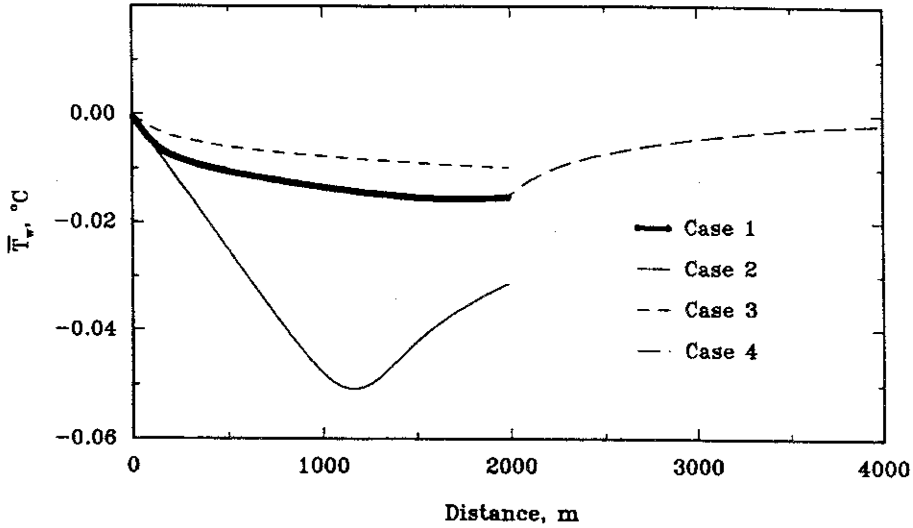

Figure 9: Variations of depth-averaged water temperature along the channel.

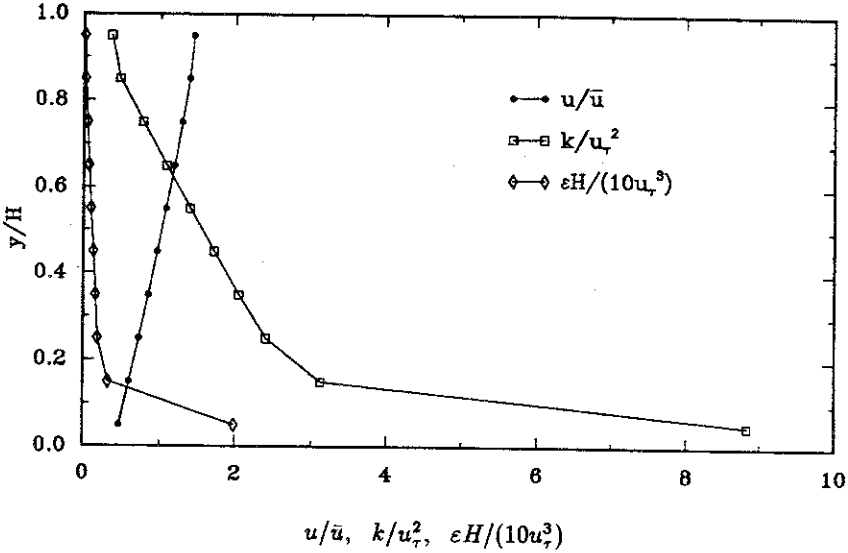

Figure 10: Vertical distributions of turbulence quantities.